ASIAN AND BARRIER OPTION PRICING PROJECT REPORT

TEAM 7

GROUP MEMBERS

YANNICK LONGVAL (1007808455): Y.LONGVAL@MAIL.UTORONTO.CA
BINHE JIA (1007651710):BINHE.JIA@MAIL.UTORONTO.CA
JINRUI HU(1008185045):JINRUI.HU@MAIL.UTORONTO.CA
JOHANNES KEHRBERGER (1012881892):JOHANNES.KEHRBERGER@MAIL.UTORONTO.CA

University of Toronto

2025 FALL ACT460: STOCHASTIC METHODS FOR FINANCE

Contents

Abstract

In this project, we investigate different aspects of Asian and barrier option, including their pricing, simulations, and behaviors. We observed that Strike or Baseline and volatility have the greatest impact on our Asian call option price and that this price is always lower and admits lower variance compared to the European call option, confirming our intuition. We analyze the impact of our simulation and discretisation methods and observe the limitations of our Monte-Carlo approach. We also compared numerical methods for estimating the greeks of the Asian call option, and conclude pathwise estimation is more accurate than finite differences.

Introduction

The purpose of this project is to analyze the prices of a number of path-dependent options and compare the closed-form solutions with numerical solutions derived from Monte Carlo simulations. Path-dependent options include Asian options, barrier options, and lookback options, which have gained popularity in financial markets because the payoff is dependent on the path followed by the underlying asset rather than just the terminal value of the asset. This implies that the mathematical tools used in the valuation of a European option may be inadequate for these types of options.

First, we come back to the geometric Brownian motion model, which will be the base for the entire discussion. The beginning of the project is centered on understanding GBM in terms of the risk-neutral probability measure, including its average, variance, and probability distribution. This is altogether essential for the construction of an options' pricing equation and comprehension of why some options qualify for a closed-form solution.

One of the main themes of the project is the comparison of solutions derived analytically from the theoretical characteristics of GBM with Monte Carlo option price estimators, which compute option prices directly from the definition of the payoff function without reference to the actual probability distributions. This comparison enables us to validate both the analytic solutions' accuracy and the Monte Carlo solutions' numerical performance.

We then explore the Greeks for the artihmetic average asian call option, and estimate delta, vega, and rho for the option using numerical methods. We use two approaches to estimate the Greeks: finite differences, and pathwise estimators. After developing each approach, we compare the results from each method to see which approach gives more accurate results.

Derivation of the closed-form solution for geometric average Asian call options will be carried out in Question 5. This is done by proving a geometric average of a GBM is itself lognormally distributed with specific drift and volatility parameters and verifying the closed-form solution with a Monte Carlo experiment, analyzing the convergence of the estimator with an increasing number of monitoring points.

Question 6 focuses on barrier options. A particular type of barrier option is chosen, and both its financial interpretation and applications will be examined. A Monte Carlo numerical solution will be established, and the generated price will be contrasted with the mathematical solution. This will emphasize the effect of discretization errors on the detection of barrier times and how increased discretization can enhance the solution's accuracy. This project covers both theoretical derivation and computational experimentation with

the objective of forming a holistic understanding of the pricing techniques used for path-dependent derivatives. Through both theoretical and numerical analysis, it is possible to appreciate both the strengths and weaknesses of the two and the contexts in which each works best.

1 Question 1: Arithmetic Average Asian Call Option

For question 1, we are going to estimate the price of an arithmetic-average Asian call option under the Black–Scholes model using Monte Carlo simulation. As the arithmetic average of correlated lognormal prices does not have a closed-form distribution, Monte-Carlo is applied to approximate the expected discounted payoff. We simulate 10,000 GBM paths with 100 time steps under the given parameters:

$$S_0 = 100, \qquad K = 100, \qquad r = 0.05, \qquad \sigma = 0.4, \qquad T = 1.$$

for the Asian call option payoff given as:

$$(\overline{S} - K)_+, \quad \text{where} \quad \overline{S} = \frac{1}{m}\sum_{i=1}^{m} S_{t_i}.$$

1.1 Black-Scholes

Let S_t be a SP modeling the stock price of a risky asset according to a GBM, i.e.

$$dS_t = rS_t dt + \sigma S_t dW_t.$$

The S_t can be expressed as

$$S_t = S_0 \exp\left(\left(r - \frac{\sigma^2}{2}\right)t + \sigma W_t\right).$$

We want to estimate the price of an Asian call option

$$(\overline{S} - K)_+, \quad \overline{S} = \frac{1}{m}\sum_{i=1}^{m} S_{t_i}.$$

According to the Black-Scholes Model, the arbitrage free price at time t can be obtained via

$$f(t, s) = e^{-r(T-t)}\mathbb{E}[F(\overline{S})|S_t = s]$$

where S_t follows the risk-free dynamics. The price of the option is then given as $f(0, S_0)$. This yields the expression

$$
\begin{aligned}
f(0, s_0) &= e^{-r(T-0)}\mathbb{E}[F(\overline{S})|S_0 = s_0] \\
&= e^{-rT}\mathbb{E}\left[\left(\frac{1}{m}\sum_{i=1}^{m} S_{t_i} - K\right)_+\right]_{S_0=s_0} \\
&= e^{-rT}\mathbb{E}\left[\left(\frac{1}{m}\sum_{i=1}^{m} S_0 \exp\left(\left(r - \frac{\sigma^2}{2}\right)t_i + \sigma W_{t_i}\right) - K\right)_+\right]_{S_0=s_0} \\
&= e^{-rT}\mathbb{E}\left[\left(\frac{s_0}{m}\sum_{i=1}^{m} \exp\left(\left(r - \frac{\sigma^2}{2}\right)t_i + \sigma W_{t_i}\right) - K\right)_+\right] \\
&= e^{-rT}\mathbb{E}\left[\left(\frac{s_0}{m}\sum_{i=1}^{m} \exp\left(\sum_{j=0}^{i}\left(r - \frac{\sigma^2}{2}\right)(t_j - t_{j-1}) + \sigma(W_{t_j} - W_{t_{j-1}})\right) - K\right)_+\right]
\end{aligned}
$$

This expression can be written for a fixed $\Delta t = t_j - t_{j-1}$ and $Z_{j+1} \sim \mathcal{N}(0, \Delta t)$ as

$$f(0, s_0) = e^{-rT}\mathbb{E}[(\frac{s_0}{m}\sum_{i=1}^{m}\exp(\sum_{j=0}^{i}(r - \frac{\sigma^2}{2})\Delta t + \sigma\sqrt{\Delta t}Z_{j+1}) - K)_+] \tag{1}$$

We cannot compute the expectation of F analytically (as it consists of a sum of correlated log-normal RV and a non-linear transformation). Nevertheless, we can obtain the following quantities

$$\mathbb{E}[\overline{S}] = \mathbb{E}[\frac{1}{m}\sum_{i=1}^{m} S_{t_i}] = \frac{1}{m}\sum_{i=1}^{m}\mathbb{E}[S_{t_i}] = \frac{s_0}{m}\sum_{i=1}^{m} e^{(r-\sigma^2/2)t_i + \sigma^2/2t_i} = \frac{s_0}{m}\sum_{i=1}^{m} e^{rt_i} \tag{2}$$

$$
\begin{aligned}
t_i \geq t_j : \ \mathbb{E}[S_{t_i}S_{t_j}] &= \mathbb{E}[s_0 e^{(r-\frac{\sigma^2}{2})t_i + \sigma(W_{t_j} + (W_{t_i} - W_{t_j})} s_0 e^{(r-\frac{\sigma^2}{2})t_j + \sigma W_{t_j}}] \\
&= s_0^2 e^{(r-\frac{\sigma^2}{2})(t_i+t_j)}\mathbb{E}[e^{\sigma(2W_{t_j} + (W_{t_i} - W_{t_j})}] \\
&= s_0^2 e^{(r-\frac{\sigma^2}{2})(t_i+t_j)} e^{2\sigma^2 t_j + (t_i - t_j)\frac{\sigma^2}{2}} \\
&= s_0^2 e^{r(t_i+t_j)+\sigma^2 t_j} \\
&= s_0^2 e^{r(t_i+t_j)+\sigma^2 \min(t_i,t_j)}
\end{aligned}
$$

$$Cov(S_{t_i}S_{t_j}) = s_0^2 e^{r(t_i+t_j)}(e^{\sigma^2 \min(t_i,t_j)} - 1)$$

$$\text{Var}(\overline{S}) = \frac{1}{m^2}\sum_{i,j=1}^{m} Cov(S_{t_i}S_{t_j}) = \frac{s_0^2}{m^2}\sum_{i,j=1}^{m} e^{r(t_i+t_j)}(e^{\sigma^2 \min(t_i,t_j)} - 1) \tag{3}$$

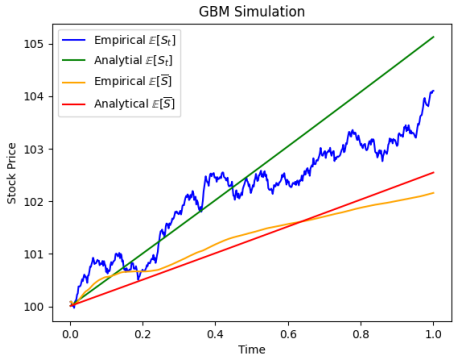

(a) Comparison for $N = 10^3$ paths

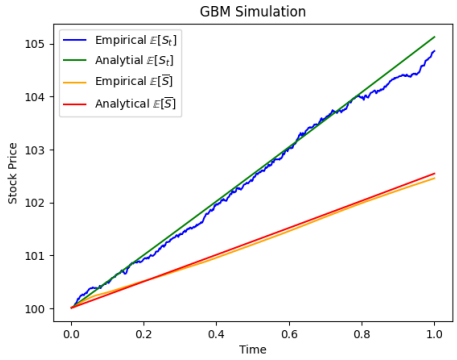

(b) Comparison for $N = 10^4$ paths

Figure 1: Comparison of analytical and empirical expectation

1.2 Monte-Carlo Simulation

To estimate the option price, we use Monte-Carlo approximation. For that, we use equation (1) which can be implemented efficiently by simulating Z as a $N \times m$ random matrix with normally i.i.d. entries and using `np.cumsum` (see implementation). Here N is the number of samples and m is the number of time steps in the average. We then multiply the discount factor with our vector containing all simulations and average over the entries to obtain the Monte-Carlo price. This $N \times m$ matrix is then averaged over the second dimension to obtain $\overline{S}$ for every simulated path and the negative entries are set to 0 leaving us with a vector with N non-negative entries.

For every approximation, the calculated value and the confidence interval is computed. The confidence interval is obtained by using the fact that the MC estimator $\hat{P}_N$ follows the distribution $\mathcal{N}(P, \frac{\sigma_X^2}{N})$ due to the CLT[1].

To check our simulation, implementation and derivation, we compare the empirical Monte-Carlo expectation of the GBM with the analytical moments derived earlier (see Figure 1).

1.3 Result and Interpretation

Computing the MC estimate we obtain an approximated option price of 9.75 ± 0.32 for $m = 100, N = 10^4$ with the given parameters. Figure 2a illustrates the GBM simulations

[1] see also Glasserman Appendix A.2

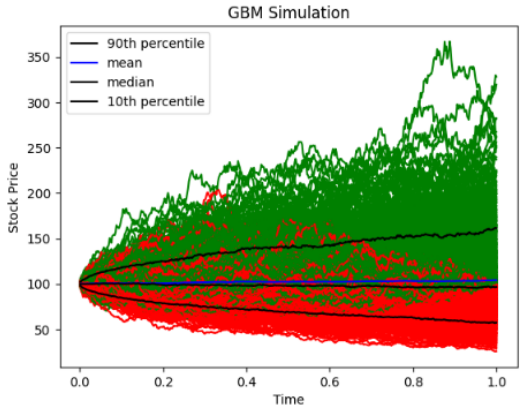

(a) GBM Monte-Carlo simulation paths

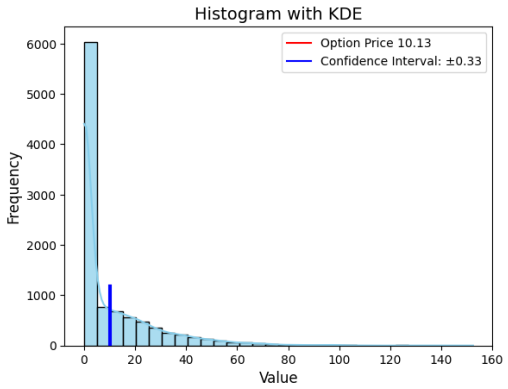

(b) Empirical payoff distribution

Figure 2: Simulation paths and distribution for Asian call option

and corresponding quantiles, where green paths have an average greater than K and red paths result in 0 payoff. To analyze the discounted payoff, we looked at its distribution, specifically at the histogram and its kernel density estimate (KDE) obtained through the simulations. We see that there is significant positive skewness in the distribution with the most mass sitting at 0, as would have been expected due to the nature of the call options payoff function. The function $\max(\bar{S} - K, 0)$ is convex and has zero as lower bound. The distribution is heavy tailed, non-gaussian, asymmetric and lives on $\mathbb{R}_{\geq 0}$. The red line represents the approximation of the option price, while the blue lines represent the confidence intervals (see Figure 2b). We expect a similar distribution as for the European call. Our analysis in section 3 shows that the distributions are structurally similar but differ on two important metrics due to their nature.

For our price calculation we used $m = 100, N = 10^4$, however as we have seen before, due to the distribution of our estimator our price is sensitive to the number of samples. Depending on the number of samples, the price approximation varies. Increasing the number of samples of our MC estimator decreases the variance in $O(1/N)$ (see distribution of $\hat{P}_N$) and thus we converge a.s. towards the real value as stated by the law of large numbers (see Figure 3). For $N = 10^5$ we obtain a price of 10.22 ± 0.12. Although for small sample sizes a large variance is present leading to uncertain approximations and big variations from the real value, due to the stochastic nature, there is always a chance of small samples performing better than larger samples. Nevertheless, a smaller number of paths is for the most part sufficient while being computationally cheap. We therefore chose $N = 5 \cdot 10^3$ for the parameter variations and the same random seed for all experiments. This helps to keep the computation cost low while producing comparable and reproducible results.

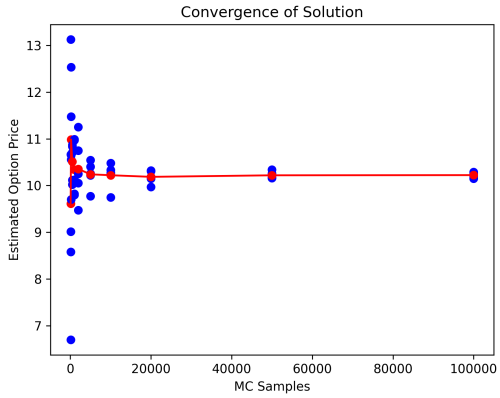

Figure 3: Convergence of the MC estimator

2 Question 2: Effects Of Model Parameters On The Price Of The Asian Option

For Q1 the following parameters were given

$$S_0 = 100,\ K = 100,\ r = 0.05,\ \sigma = 0.4,\ T = 1.$$

We varied each of the parameters and analyzed their impacts on the price. Furthermore, we compared the effects to the European call option. We used $N = 5000$ Monte Carlo path simulations per run with $m = 100$ time check-points.

2.1 Variation of baseline S_0

When we vary the Baseline S_0 we directly influence the payoff function as the GBM is constructed upon S_0. When we increase the baseline the asset price will be higher on average than in the standard case. This makes the asset and thus the call option more valuable, which increases the option price. In the empirical distribution of the payoff we see a shift caused by the shift in S_0 (see Figure 4). The in-the-money probability increases as the cut-off of the payoff function is less frequent. Payoff and sample-mean scale with S_0 (see Figure 5a).

For large differences between S_0 and K, the dependency between price and baseline is almost linear but it becomes convex around the area where S_0 and K are close to each other (see Figure6).

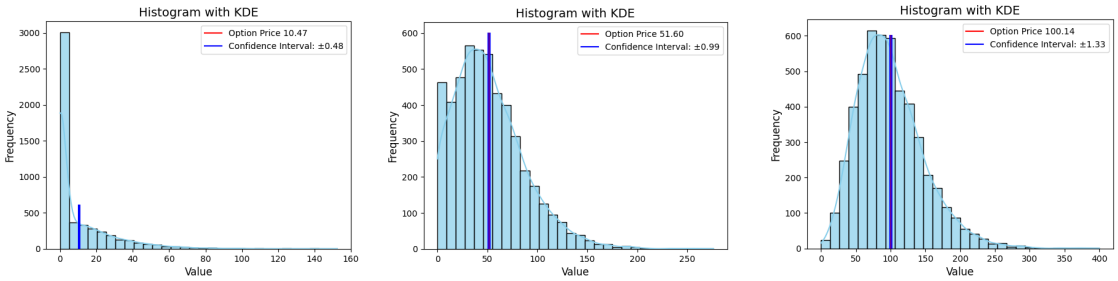

(a) Base case for $S_0 = 100$ (b) Case for $S_0 = 150$ (c) Case for $S_0 = 200$

Figure 4: Shift of the distribution with shift of S_0

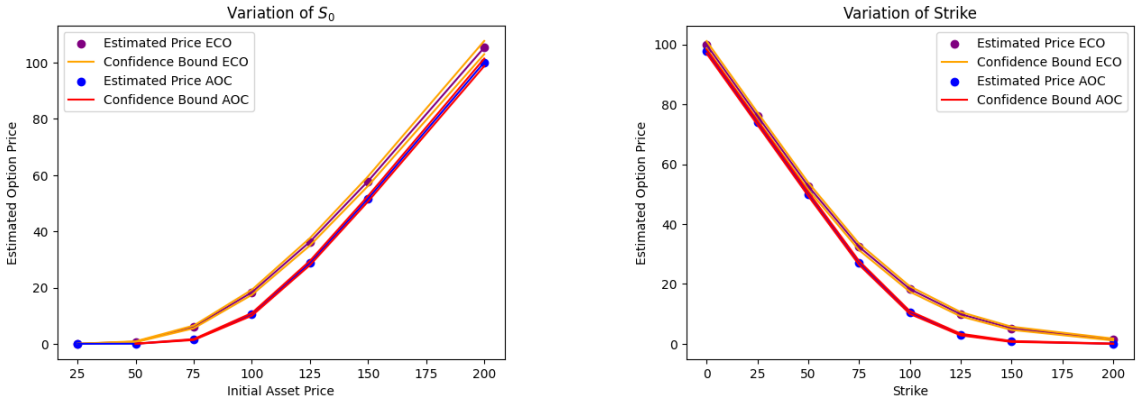

(a) Evolution of price with S_0 (b) Evolution of price with K

Figure 5: Evolution of price with payoff parameter

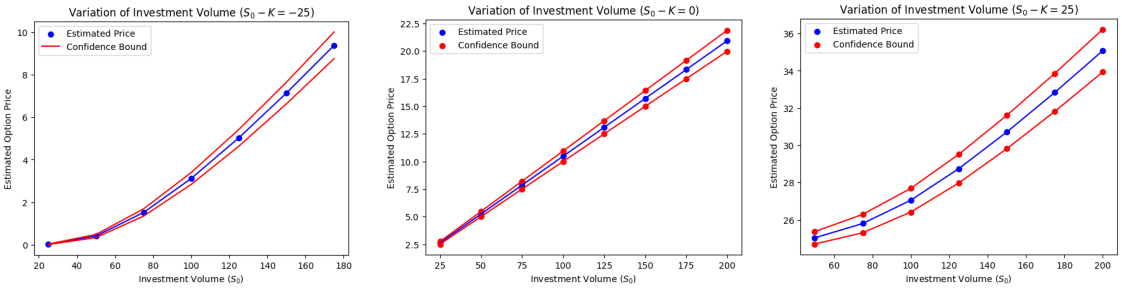

(a) Base for $S_0 - K = -25$ (b) Case for $S_0 - K = 0$ (c) Case for $S_0 - K = 25$

Figure 6: Behavior for different Baseline - Strike discrepancies

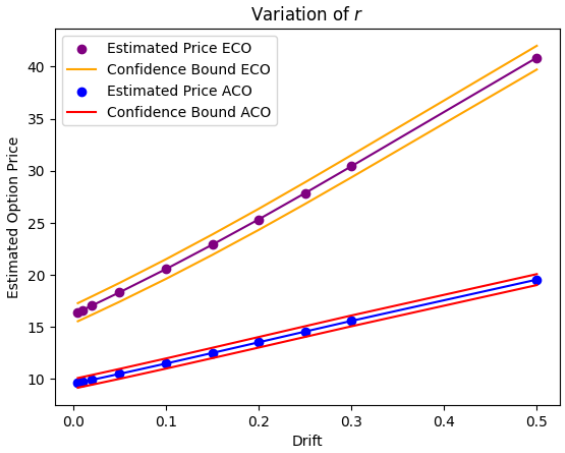

Figure 7: Evolution of price in r

2.2 Variation of strike K

Varying the strike price K varies the threshold of the payoff which directly impacts the probability of ending up in or out of the money. Increasing K makes it more unlikely to reach the threshold and thus making the option less valuable. The strike directly impacts the variance and mean as the distribution clusters around 0 if the strike price is too high and spreads out if the discrepancy between S_0 and K becomes smaller than S_0 (see Figure 5b). We can see a directly opposing behavior between S_0 and K (see Figure 5).

2.3 Variation of drift r

The parameter r is defining the drift of the GBM as well as the discount factor. By varying r we therefore get opposing effects that act on the GBM and thus the price. A higher drift r increases the upward trend of the asset, which raises the expectation of the mean. The option price increases monotonically but slowly in r, showing that the drift dominates the discount factor, though the discount partially offsets this effect. Higher drift increases the tendency of the option to end up in-the-money, but the effect is dampened by the averaging nature of the option (see Figure 7). In practice, it seems reasonable to assume $r \in [0, 1]$. If we look, however, at large r for theoretical purposes, we see that the discount factor becomes increasingly influential, to the point where it fully dominates the behavior (see Figure 8). For $r \to \infty$ we therefore get $f(0, s_0) \to 0$. Similar to the observations later seen for σ, the almost linear behavior for small values changes to a exponential behavior for large values. These large values however are mostly not relevant in practice.

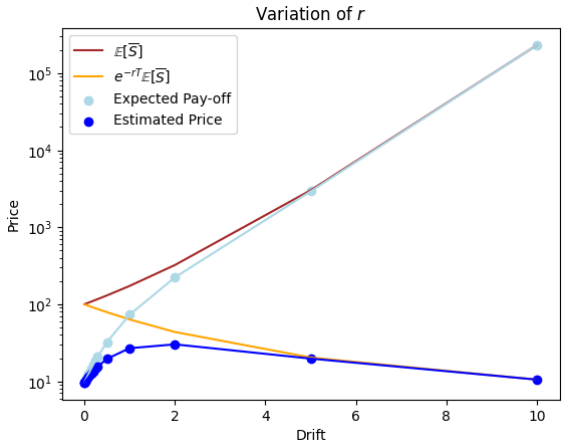

Figure 8: Dominating factors in the price evolution r

2.4 Variation of volatility σ

Changing the parameter σ changes the volatility of the asset. This increases not the number of in-the-money paths but the number of paths that end up with a very high asset value. As the payoff only depends on the in-the-money outcomes, the option price increases. However, due to the averaging nature of the option, volatility gets dampened compared to the European call (see Figure 9b).

As σ gets larger, i.e. $\sigma > 1$ the underlying GBM is dominated by $e^{\sigma W_t}$, forcing an exponential behavior which does not exist for small σ. This leads to a non-linear behavior in this area other than the nearly linear behavior for small σ, where the behavior is dominated by e^{rt} (see $\mathbb{E}[\overline{S}]$ and Figure 9a)

2.5 Comparison to the European call option

The European call option is only determined by the value of the asset at maturity, whereas the value of the Asian call option is determined by the average of the price over time. This averaging has some interesting effects that separate these two options significantly. We saw in the analysis that the averaging always decreases the price compared to the European call option (see f.e. Figure 7) and also decreases the uncertainty of the outcome (see f.e. Figure 9b). Intuitively we expect to see that averaging decreases uncertainty as also values at earlier time steps are taken into account for which the uncertainty is lower than for large time steps. Furthermore, averaging also decreases the compounding effect

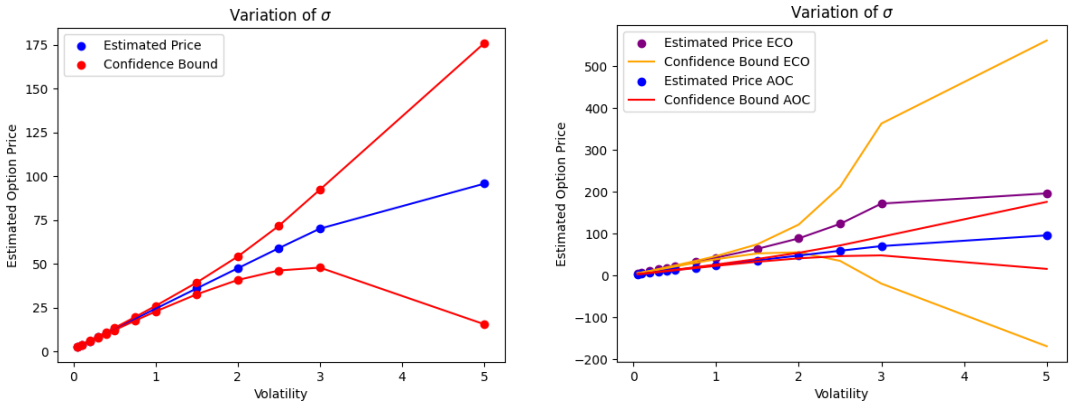

(a) Dependency between price and σ (b) Comparison of Asian and European call

Figure 9: Evolution of price in σ

leading to a lower expected payoff and thus a lower option price.

Mathematically we see that

$$\begin{aligned}
\text{Var}(\overline{S}) &= \frac{s_0^2}{m^2} \sum_{i,j=1}^{m} e^{r(t_i+t_j)} (e^{\sigma^2 \min(t_i,t_j)} - 1) \\
&< \frac{s_0^2}{m^2} \sum_{i,j=1}^{m} e^{rT} (e^{\sigma^2 T} - 1) \\
&= s_0^2 e^{2rT} (e^{\sigma^2 T} - 1) \\
&= \text{Var}(S_T)
\end{aligned}$$

and also

$$\mathbb{E}[\overline{S}] = \frac{s_0}{m} \sum_{i=1}^{m} e^{rt_i} < \frac{s_0}{m} \sum_{i=1}^{m} e^{rT} = s_0 e^{rT} = \mathbb{E}[S_T]$$

where we use $T = t_m$ and equations (2) and (3) from section 1. We see that $\text{Var}(\overline{S}) < \text{Var}(S_T)$ and $\mathbb{E}[\overline{S}] < \mathbb{E}[S_T]$ which directly translates to the payoff and confirms our intuitive and financial understanding. These results can also be seen when comparing the empirical payoff distributions for both options in Figure 10, where blue corresponds to the Asian option and orange to the European option.

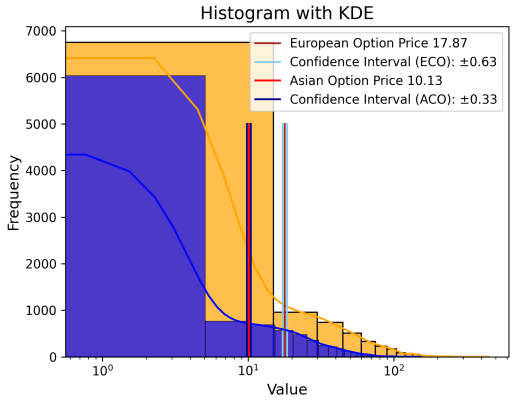

Figure 10: Comparison of payoff distributions (x log-scale)

3 Question 3: Effect of Discretization Errors

In addition to the effects of the parameters on the price it is of interest to asses the effect that the discretization has on our simulations. As the underlying asset can be modeled by a GBM, there is no need to compute the asset evolution using any approximation schemes for our analysis. The GBM has an analytical solution, thus using schemes like Euler, Milstein, etc. can only give worse results as these discretization methods introduce new approximation errors. Due to that fact, examining different Δt for the GBM and the averaging gives us no improvement as evaluation the GBM on a finer time mesh adds no accuracy. Therefore the only interesting variation in the discretization is the one of m.

3.1 Variation of m

Our underlying asset admits an analytical solution for its underlying SDE, however, as our asset always has a continuous path, the value $\overline{S}$ encounters a discretization error, as it only captures a finite number of points in time. For $m \to \infty$, $\overline{S}$ can be expressed as $\frac{1}{T}\int_0^T S_t dt$ path wise. Using this continuous average we can look at the impact of m on the price and also use the trapezoidal rule as a better numerical integration for the average. It is important to note that due to the implementation, approximations on larger m's wont admit the same values on their common time reference points, as the normally distributed matrix used for the GBM will not be the same for different m even when using the same random seed. A direct comparison would require a careful adaptation of the code which makes sure that the common time points use the same realization of the normal random variable. To circumvent this problem and to keep the code more efficient and applicable to

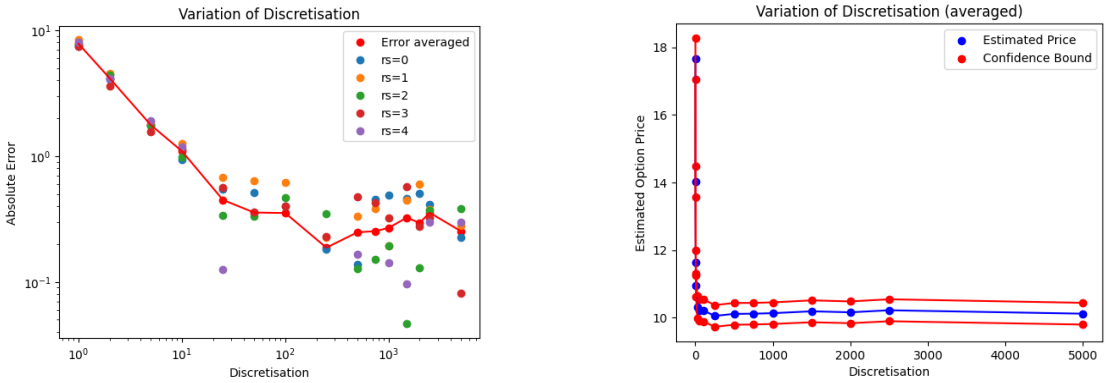

(a) Error evolution log-log plot

(b) Price vs. m averaged

Figure 11: Variation of the number of time steps

other tasks, we use multiple seeds and average our results. Due to the sampling approach in general this should not modify the results significantly.

To analyze the error, we computed a reference solution with $m = 10^4$ time points using the trapezoidal rule explained later. After computing the price for different m we obtained Figure 11b. We can see that similar to the comparison for the number of Monte-Carlo paths, our price converges. In this case it converges with respect to the continuous average whereas in N it converged with respect to the expectation. Comparing our price with the reference solution we see a empirical order of convergence (EOC) of around -1 for small m which changes to roughly -0.5 for moderate m. We expect to see an EOC of -1 due to the convergence order of the sum. The effects that change the EOC for increasing m are most likely due to the GBM and the simulation approach. For large m we see a fluctuating pattern. To see what causes this behavior, we computed the results for multiple random seeds. The plots show that the fluctuations for large m are caused by the Monte-Carlo noise which dominate the error in this area (see Figure 11a). It has to be stated that the error analysis is very limited and an often not be made very rigorous due to the stochastic nature of the problem and reference solutions.

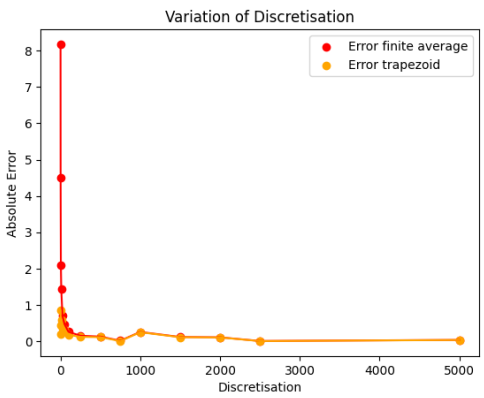

(a) Error vs. number of time steps

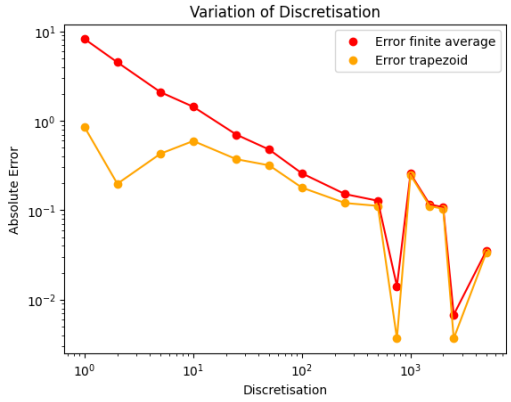

(b) Error evolution log-log plot

Figure 12: Error comparison trapezoidal rule and finite average

3.2 Comparison to the trapezoidal rule

The finite average depicted in the task is a Riemann-sum approximation of the continuous average (using $t_i - t_{i-1} = \Delta t = const.$)

$$\frac{1}{T}\int_0^T S_t \mathrm{d}t \approx \frac{1}{T}\sum_{i=1}^{m} S_{t_i}\Delta t = \frac{1}{m}\sum_{i=1}^{m} S_{t_i}$$

Choosing a better method of numerical integration therefore should give us a better result. We chose the trapezoidal rule for comparison, i.e.

$$\frac{1}{T}\int_0^T S_t \mathrm{d}t \approx \frac{1}{T}\sum_{i=1}^{m} \frac{S_{t_i} + S_{t_{i-1}}}{2}\Delta t = \frac{S_0 - S_T}{2m} + \frac{1}{m}\sum_{i=1}^{m} S_{t_i}$$

What can be observed is, that for small m the trapezoidal rule always performs better as expected. However, for large m, both methods perform very similar (see Figure 12). As seen in the prior analysis, the Monte-Carlo noise become very dominant for large m making it hard to analyze the EOC and error behavior. Depending on the use case, computational resources and the concrete structure of the option, i.e. continuous or discrete average, choosing a better integration method might be a good decision. Nevertheless, our analysis shows that even $m = 100$ can be sufficiently large to justify using the discrete average proposed in the question, depending on the desired accuracy.

4 Question 4: Greeks

4.1 Estimation Methods

This section uses numerical methods for estimating the delta $\frac{\partial Y}{\partial S_0}$, the vega $\frac{\partial Y}{\partial \sigma}$, and the rho $\frac{\partial Y}{\partial r}$, for the arithmetic average asian call option. We explore two methods for estimating the greeks: finite differences and pathwise estimators.

4.2 Finite Differences

The finite differences approach for estimating the greeks is done by slightly offsetting the corresponding parameter by a small value h, and calculating the rate of change of the option price (Y) after offsetting the parameter. This calculation is shown below, for some parameter θ.

$$\frac{\partial Y}{\partial \theta} = \frac{Y(\theta + h) - Y(\theta)}{h} \tag{4.1}$$

There are a few methods to simulate with the finite differences approach. The method shown in expression (4.1) describes the forward differences method. An alternative method is using central differences, which is shown in expression (4.2) below.

$$\frac{\partial Y}{\partial \theta} = \frac{Y(\theta + h) - Y(\theta - h)}{2h} \tag{4.2}$$

The central differences method further offsets the parameter by $-h$, such that the orignal parameter is centered between both offsets, and calculates the difference in option price from both offsets.

In addition to forward differences vs central differences, the finite differences approach can use independent draws or Common Random Numbers (CRN). Independent draws is performed by simulating $Y(\theta)$ and $Y(\theta+h)$ independently of eachother, whereas CRN re-suses the same random variables when simulating the option price. Since CRN causes the covariance of the offsetted and base simulations to be non-zero, the variance of the CRN will inherently be smaller than the independent method. We simulate all 4 combinations of (forward differences, central differences) x (independent draws, CRN) in section 4.3, to show the difference in variance.

4.3 Pathwise Estimators

The pathwise estimators approach aims to estimate the greeks by developing an expression directly for the derivative:

$$\frac{\partial Y}{\partial \theta} = \frac{\partial}{\partial \theta}\mathbb{E}\left[Y\right]$$

Note that the Y in $\mathbb{E}\left[Y\right]$ denotes the simulated option price, which we simulate the expectation of using Monte Carlo. For us to further simulate the derivative using Monte Carlo, the following expression must hold:

$$\frac{\partial}{\partial \theta}\mathbb{E}\left[Y\right] = \mathbb{E}\left[\frac{\partial Y}{\partial \theta}\right] \tag{4.3}$$

For the paramters that we are observing (S_0, σ, and r), the option price Y is differentiable at all points expect when $\bar{S} - K = 0$. However, the probability of the single point $\bar{S} - K = 0$ is 0, and thus Y is almost surely differentiable, and (4.3) holds.

Since (4.3) holds, we can simulate the derivative directly with Monte Carlo, and average the simulations to get an expectation. The expressions for each greek that we'll estimate in our simulations are shown below (for the derivation of each expression, please see Appendix):

Delta:

$$\boxed{\frac{\partial Y}{\partial S_0} = e^{-rT}1\{\bar{S} > K\}\frac{\bar{S}}{S_0}}$$

Vega:

$$\boxed{\frac{\partial Y}{\partial \sigma} = e^{-rT}1\{\bar{S} > K\}\frac{1}{m}S_0\sum_{i=1}^{m} e^{(r-\frac{1}{2}\sigma^2)t_i+\sigma W_{t_i}}[-\sigma t_i + W_{t_i}]}$$

Rho:

$$\boxed{\frac{\partial Y}{\partial r} = e^{-rT}[-T[\bar{S} - K]^+ + 1\{\bar{S} > K\}\frac{1}{m}S_0\sum_{i=1}^{m} t_i e^{(r-\frac{1}{2}\sigma^2)t_i+\sigma W_{t_i}}]}$$

4.4 Result

The results we observe in this section are for the arithmetic average Asian call option with the following parameters:

$$S_0 = 100, \qquad K = 100, \qquad r = 0.05, \qquad \sigma = 0.4, \qquad T = 1$$

Furthermore, we performed our Monte Carlo (MC) simulations with $n = 2000$ simulations per MC, 1000 timestamps per simulation ($t = \frac{1}{1000}$), and $h = 0.01$ for the finite differences approach.

We ran MC for each greek, for each configuration of the finite differences (FD), as well as the pathwise estimator (PW), for a total of 15 MC simulations.

The results of the simulations for each greek are displayed through three tables. Each table also includes the standard error and confidence intervals for each simulation.

Delta:

	Estimate	**Standard Error**	**Confidence Interval (95%)**
FD, Forward, Independent	16.44	52.06	[-85.6, 118.47]
FD, Forward, CRN	0.57	0.01	[0.54, 0.59]
FD, Central, Independent	-36.42	27.15	[-89.64, 16.8]
FD, Central, CRN	0.57	0.01	[0.54, 0.59]
PW	0.56	0.01	[0.54, 0.59]

Table 1: Delta Result

Vega:

	Estimate	**Standard Error**	**Confidence Interval (95%)**
FD, Forward, Independent	23.86	53.73	[-81.46, 129.17]
FD, Forward, CRN	21.67	1.08	[19.55, 23.78]
FD, Central, Independent	34.35	25.55	[-15.73, 84.43]
FD, Central, CRN	22.92	1.08	[20.81, 25.03]
PW	20.52	0.96	[18.63, 22.4]

Table 2: Vega Result

Rho:

	Estimate	Standard Error	Confidence Interval (95%)
FD, Forward, Independent	55.01	52.72	[-48.33, 158.35]
FD, Forward, CRN	20.20	0.46	[19.3, 21.09]
FD, Central, Independent	36.08	25.75	[-14.39, 86.55]
FD, Central, CRN	19.12	0.45	[18.24, 20.01]
PW	19.71	0.46	[18.8, 20.62]

Table 3: Rho Result

From the results, it is clear that the independent draws method for the FD approach produces much larger standard errors than the other methods. Additionally, the CRN methods for the FD approach are very close to the pathwise estimator approach, which is more clearly shown in the following tables which compare the differences between the FD methods and the pathwise estimator.

Delta:

	FD Estimate	PW Estimate	Difference
FD, Forward, Independent	16.44	0.56	15.87
FD, Forward, CRN	0.57	0.56	0
FD, Central, Independent	-36.42	0.56	-36.99
FD, Central, CRN	0.57	0.56	0

Table 4: Delta Difference

Vega:

	FD Estimate	PW Estimate	Difference
FD, Forward, Independent	23.86	20.52	3.34
FD, Forward, CRN	21.67	20.52	1.15
FD, Central, Independent	34.35	20.52	13.83
FD, Central, CRN	22.92	20.52	2.40

Table 5: Vega Difference

Rho:

	FD Estimate	PW Estimate	Difference
FD, Forward, Independent	55.01	19.71	35.3
FD, Forward, CRN	20.20	19.71	0.49
FD, Central, Independent	36.08	19.71	16.37
FD, Central, CRN	19.12	19.71	-0.59

Table 6: Rho Difference

To conclude our analysis of the greeks, we compare the Kernel Density Estimate (KDE) of the simulations using finite differences to pathwise estimators. We see that the KDE of the pathwise estimators are overall more concentrated than the finite differences, which is discerned by the taller peaks of the pathwise KDE. Note that only the central differences/CRN method for finite differences is shown, as the other methods follow similarly/more strongly justify our observation.

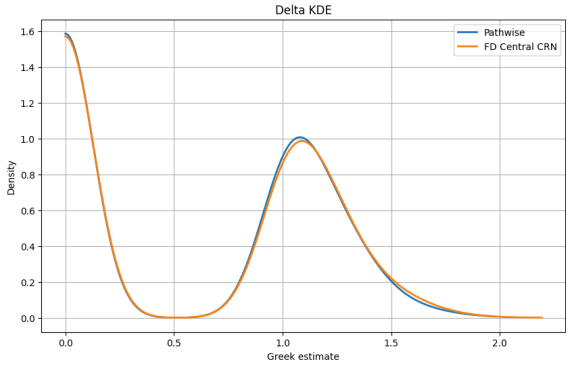

Figure 13: Kernel Density Estimate of simulated delta estimates

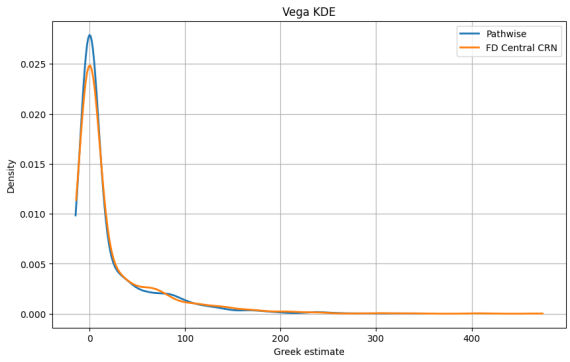

Figure 14: Kernel Density Estimate of simulated vega estimates

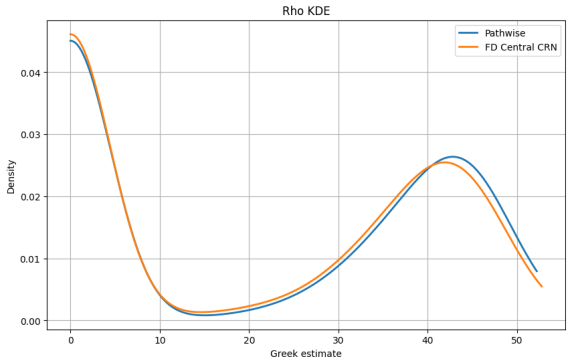

Figure 15: Kernel Density Estimate of simulated rho estimates

Thus, we conclude that pathwise estimators produce more concentrated, and thus more stable, estimates of the greeks than the finite differences approach. Intuitively this makes sense, as the pathwise estimator uses more information about the option, and relies on additional assumptions to develop an expression for the derivative. Within the finite difference methods, the common random numbers methods produce more accurate results than the independent draws methods.

5 Question 5: Geometric Average Asian Call Option

5.1 Derivation of the Closed-Form Formula for the Geometric Average Asian Call

For Question 5, our objective is to derive the closed-form pricing formula for a geometric Asian option and then verify this formula using Monte Carlo simulations. Also, the purpose of this derivation is to show that the geometric average of a GBM is follows lognormal distribution. Once we confirmed that it is lognormal, the pricing of a geometric Asian call reduces to applying the Black Sholes with adjusted drift and volatility parameters.

We begin with the definition of the geometric average of the underlying asset. For monitoring dates $t_1, \ldots, t_m$, the geometric average is defined as

$$\bar{S} = \left(\prod_{i=1}^{m} S_{t_i} \right)^{1/m}$$

Before substituting into the geometric average, we first recall the closed-form solution of a geometric Brownian motion (GBM). A GBM satisfies

$$S_t = S_0 \exp\big((r - \tfrac{1}{2}\sigma^2)t + \sigma W_t\big)$$

which allows us to write each monitoring value S_{t_i} in exponential form.

Then, the key step is taking logarithms: since $\log S_t$ is normally distributed for a GBM, the log of the geometric average becomes a linear combination of normal random variables, and therefore remains normal.

Since a GBM satisfies

$$\log S_t \sim N\big(\log S_0 + (r - \tfrac{1}{2}\sigma^2)t,\ \sigma^2 t\big)$$

each $\log S_{t_i}$ is normally distributed, and any linear combination of normal variables remains normal. Thus,

$$\log \bar{S} = \frac{1}{m} \sum_{i=1}^{m} \log S_{t_i}$$

is also normal, which guarantees that $\bar{S}$ is lognormal. This property is the foundation that allows us to derive a closed-form price.

Glasserman (2004) provides the distributional result

$$\left(\prod_{i=1}^{m} S(t_i)\right)^{1/m} = S_0 \exp\left(\left[r - \tfrac{1}{2}\sigma^2\right] \frac{1}{m}\sum_{i=1}^{m} t_i + \frac{\sigma}{m}\sum_{i=1}^{m} W(t_i)\right)$$

$$and$$

$$\sum_{i=1}^{m} W(t_i) \sim N\left(0,\ \sum_{i=1}^{m}(2i-1)t_{m+1-i}\right)$$

It follows that the geometric average of $S(t_1), \ldots, S(t_n)$ has the same distribution as the value at time T of a GBM with adjusted parameters:

$$\bar{T} = \frac{1}{m}\sum_{i=1}^{m} t_i, \qquad \bar{\sigma}^2 = \frac{\sigma^2}{m^2 T}\sum_{i=1}^{m}(2i-1)t_{m+1-i}, \qquad \delta = \frac{1}{2}\sigma^2 - \frac{1}{2}\bar{\sigma}^2$$

In the continuous-monitoring case, the geometric average is

$$\exp\left(\int_u^t \log S(\tau)\, d\tau\right)$$

which is also lognormally distributed. Therefore, options on a continuous geometric average can similarly be priced in closed form.

(Reference: Glasserman (2004), *Monte Carlo Methods in Financial Engineering*, Section 3.2.)

5.2 Monte Carlo Validation of the Closed-Form Formula

Once the geometric average is shown to be lognormal, pricing the geometric Asian call reduces to applying the Black–Scholes formula with the adjusted drift and variance parameters.

Thus, we have:

$$d_+ = \frac{\ln(S_0/K) + (r - \delta + \frac{1}{2}\bar{\sigma}^2)\,\bar{T}}{\bar{\sigma}\sqrt{\bar{T}}}, \qquad d_- = d_+ - \bar{\sigma}\sqrt{\bar{T}}.$$

Then for this Asian call option, the Black-scholes closed-form is:

$$C_0 = S_0 e^{-\delta\bar{T}}\Phi(d_+) - K e^{-r\bar{T}}\Phi(d_-)$$

However, the closed-form solution that we have right now is dependent on assumptions in the theory related to the lognormal distribution of the geometric average, and the adjusted drift and volatility terms, which come from the GBM model. The Monte Carlo simulation, on the other hand, derives the option value from the definition without using the process that we used in the closed-form formula. Therefore, the Monte Carlo simulation is consider as a unbiased estimator, and the results converge to the correct mean as the number of simulations increases. Thus, we use Monte Carlo simulations to check the validity of the closed-form expression.

In Monte Carlo simulations, we approximate the option price simply from the definition by simulating a large number of sample paths using the GBM model, calculating the geometric averages at the monitoring times, and discounting the corresponding payoff values. In contrast to the closed-form solution, the Monte Carlo approach does not use any of the assumptions made in the analytical solution, like the lognormal distribution of the geometric average. Instead, it evaluates:

$$C_0 = e^{-rT}\mathbb{E}\big[(\bar{S} - K)^+\big]$$

numerically through sampling. The Monte Carlo estimator is unbiased and the approximation converges to the actual value as the number of simulated paths increases, making the Monte Carlo approach an independent check on the correctness on the closed-form solution.

In our implementation, we simulation process of the GBM under the exact solution

$$S_{t+\Delta t} = S_t \exp\Big((r - \tfrac{1}{2}\sigma^2)\Delta t + \sigma\sqrt{\Delta t}\, Z\Big)$$

with $Ndt = 252$ time steps, equivalent to about 252 trading days in a year. The geometric average in each path $j = 1, \ldots, N_{sim}$, and we use $N_{sim} = 2000$ simulated paths and select monitoring dates $m \in \{100, 200, 500, 1000, 2000\}$ aim to compute the geometric average more accurate by

$$\bar{S}_j = \exp\left(\frac{1}{m}\sum_{i=1}^{m} \log S_{t_i}^{(j)}\right)$$

and the discounted payoff is

$$\text{payoff}_j = e^{-rT}\max(\bar{S}_j - K,\, 0)$$

The Monte Carlo estimator is given by averaging payoff j over all simulated paths. The sample standard deviation serves in calculating the standard error and the 95Comparing

the simulated prices with the closed-form formula, the analytical solution always lies in the confidence interval, and the absolute error becomes smaller with the increase in the number of monitoring points. The simulation results prove the validity of the closed-form solution and the convergence of the Monte Carlo estimator to the analytical solution. Having implemented both the closed-form formula and the Monte Carlo estimator in Section 5.1 and 5.2, we now compare their numerical outputs and analyze how closely the simulation results converge to the analytical solution.

5.3 Results and Interpretation

After the calculation, for any value of m, the prices derived using Monte Carlo simulations approximate the theoretical closed-form solutions very closely: when $m = 2000$, the closed-form formula will have $C_0 = \$9.36$, and the Monte Carlo simulation will have $C_0 = \$9.46$ (table 7). More importantly, the closed-form solution is always contained within the Monte Carlo 95% confidence interval, establishing data consistency. Also, the difference between the closed-form solution and the Monte Carlo estimate tends to decrease with an increase in m (figure 16), which is consistent with the theoretical reasoning that a geometric average with a larger number of monitoring points will approximate the continuous situation better (figure 17).

Overall, the simulation results provide strong numerical evidence confirming the correctness of the closed-form pricing formula for the geometric-average Asian call. Since the Monte Carlo estimator is unbiased and converges to the true value as the number of simulations increases, the close agreement between the two methods indicates that the analytical expression is implemented and derived correctly.

	Analytic	**MC Price**	**Standard Error**	**Confidence Interval (95%)**	**Diff**
m=100	9.44	9.25	0.34	[8.58, 9.91]	0.20
m=200	9.40	9.87	0.36	[9.17, 10.56]	0.47
m=500	9.38	9.26	0.33	[8.61, 9.92]	0.18
m=1000	9.37	9.71	0.35	[9.03, 10.40]	0.34
m=2000	9.36	9.46	0.34	[8.80, 10.12]	0.09

Table 7: Analytic vs. Monte-Carlo estimates for the geometric Asian call at various monitoring frequencies.

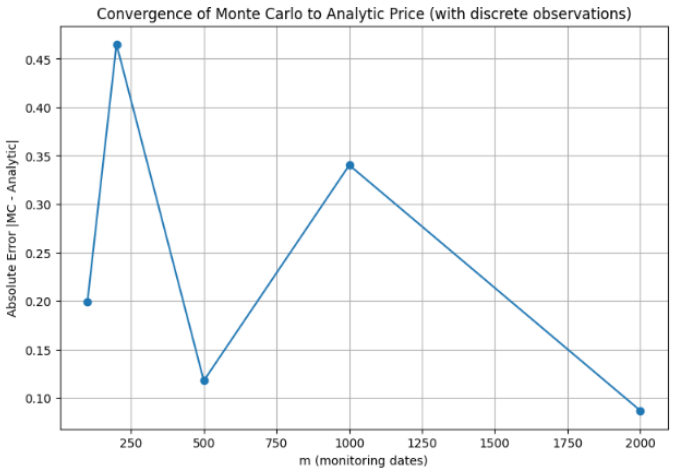

Figure 16: Convergence of the Monte Carlo estimator towards the analytical price with an increase in the number of monitoring dates. The figure above illustrates the absolute error in the Monte Carlo price and the analytical geometric Asian call price with varying values of m, thereby highlighting how the error in discretization reduces with an increase in the value of m.

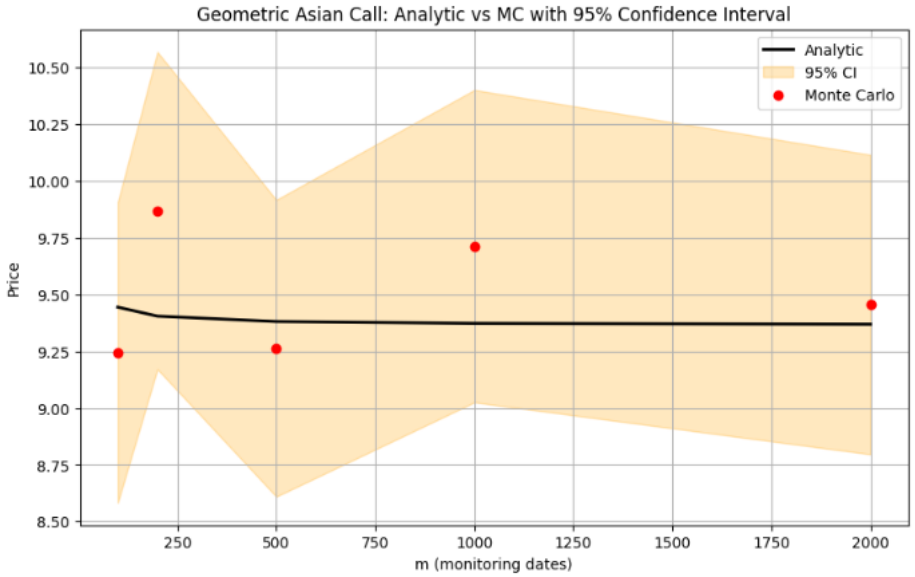

Figure 17: Analytic price compared with Monte Carlo estimates and their 95% confidence intervals across different monitoring dates

6 Question 6: Barrier Up-and-In Put Option

6.1 Introduction

A Barrier Up-and-In Put option is an exotic option that can be exercised only if the underlying asset price S_t reaches or exceeds a predetermined upper barrier $B > S_0$ at any time before maturity T. If the barrier is never hit, the option expires worthless; if the barrier is hit, then the option behaves exactly as an European put option with strike price K at maturity T (knock-in).
Formally, define $\tau_B = \inf\{t \in [0,T] : S_t \geq B\}$, which is the first hitting time of the barrier. Then an up-and-in option has the following payoff:

$$F(S_T) = (K - S_T)_+ \mathbb{I}_{\{\tau_B \leq T\}}$$

where $\mathbb{I}$ is indicator function.
Compared with a European put option, an Up-and-In Put is priced cheaper because it expires worthless if the barrier condition is not satisfied. Such options are useful when it is expected that the underlying price will rise to a known level before potentially declining before the expiry

6.2 Pricing Formula

According to Hull (Chapter 26.9), the price of an Up-and-In Put option can be obtained using the in–out parity relation:

$$P_{\text{up-in}} = P_{\text{vanilla}} - P_{\text{up-out}},$$

where P_{vanilla} is the price of a standard European put and $P_{\text{up-out}}$ is the price of an Up-and-Out Put option with the same parameters. Using this, we may derive the closed-form expression for the Up-and-In Put price given by

$$p_{ui} = -S_0 e^{-qT} \left(\frac{H}{S_0}\right)^{2\lambda} \Phi(-y) + K e^{-rT} \left(\frac{H}{S_0}\right)^{2\lambda-2} \Phi(-y + \sigma\sqrt{T}),$$

where

$$y = \frac{\ln\left(\frac{H^2}{S_0 K}\right) + (r - q + \frac{1}{2}\sigma^2)T}{\sigma\sqrt{T}}$$
$$\lambda = \frac{r - q + \frac{1}{2}\sigma^2}{\sigma^2}$$

$\Phi(\cdot)$ is the cumulative distribution function of the standard normal.
Here:

1. S_0: current price of the underlying asset,
2. K: strike price,
3. H: barrier level (with $H > S_0$),
4. r: risk-free rate,
5. q: continuous dividend yield (often 0 if none),
6. σ: volatility,
7. T: time to maturity.

Upon calculating the analytic price as well as the simulated price using Monte Carlo (time step: 252), we have the following:

- Analytic Price: 0.21
- Monte Carlo: 0.17

We noticed that Monte Carlo price tends to be lower than the analytic one. However, this is expected because the analytic price is based on continuous approach, while the Monte Carlo simulated price is an discrete approximation. Therefore, it is likely that some hitting happened might be missed when the price is approximated discretely (see figure), which leads to lower price for up-and-in option. In fact, when we increase the time step to 2000, we have

- Analytic Price: 0.21
- Monte Carlo: 0.2

which shows an significant improvement. So more time step reduces the bias caused by the discretization.

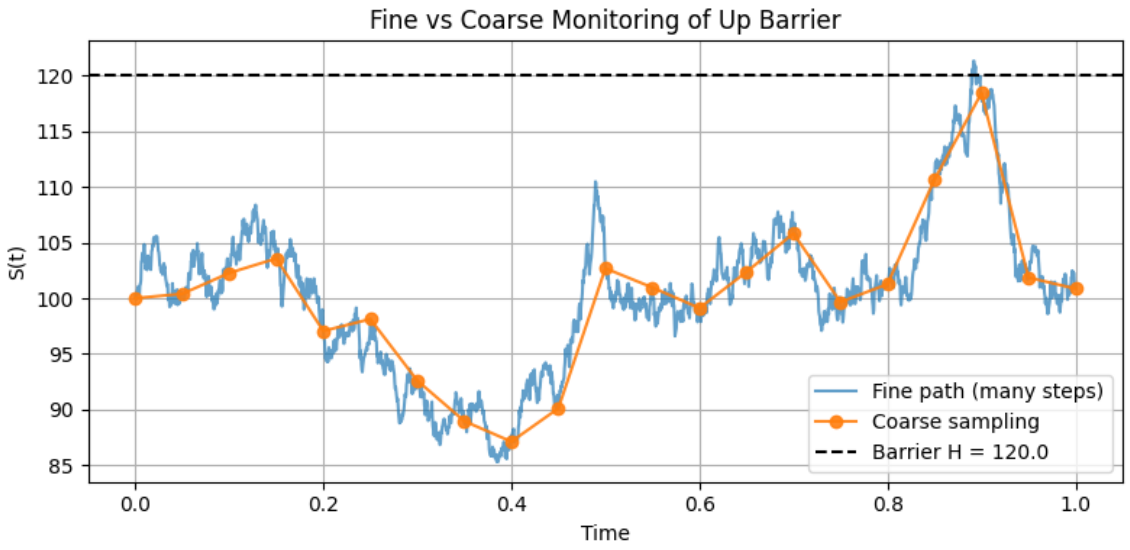

Figure 18: Comparison of coarse and fine sample paths for barrier up-and-in put. Notice that the fine path (blue) is knocked-in because it hits the barrier H at $t \approx 0.9$, whereas the coarse path (orange) fails to capture this.

7 Conclusion

In this project, we investigated the pricing of an Asian call option using the Black–Scholes model and Monte Carlo simulation and analyzed the influence of model parameters and discretization choices on the resulting option price. We validated the correctness of our implementation by comparing empirical Monte Carlo moments against their theoretical counterparts. This provided a solid foundation for the computation of the option price through Monte-Carlo simulations of the underlying asset. Our parameter study revealed several characteristic features of Asian options. Variations in the baseline S_0 and strike K had the biggest impact on the price. These two parameters showed directly opposing behavior on price and revealed that the price dynamics experience a change in the area where S_0 and K are cloes to each other. Adjusting the drift r highlighted the interaction between the upward trend in the underlying asset and the discounting of the payoff, with the drift dominating for practically relevant values. The volatility σ had a positive but moderated impact on the price, especially compared to a European option, reflecting the dampening effect of averaging on variance. In a direct comparison we saw that the averaging reduces both expected payoff and variance, and therefore systematically lowers the option price.

This is backed by theoretical results. For the analysis of the discretization we focused on the temporal average. Although the underlying GBM admits a closed-form solution, the discrete approximation of the time average introduces a numerical integration error. We looked at the behaviour for different choices of time steps and compared the standard finite average (Riemann sum) used in the assignment with a more accurate trapezoidal rule. Against a high-resolution reference solution, the finite average exhibited an empirical order of convergence of approximately -1 for small m, gradually transitioning to a value around -0.5 as Monte Carlo noise began to dominate for larger m. As expected, the trapezoidal rule improved accuracy for coarse discretizations, but both methods performed similarly once m was sufficiently large. These results suggest that the primary source of error is the stochastic sampling rather than the temporal discretization. This suggests that our pricing and analysis is limited by the limitations of the Monte-Carlo approach. A more rigorous analysis would benefit from variance-reduction techniques, shared Brownian increments across discretization levels, and potentially more advanced methods such as quasi– or multilevel Monte Carlo. Furthermore, extending the study to more realistic asset dynamics like time dependent volatility would provide additional insight into the robustness of the observed effects.

8 References

Hull, J. C. (2021). Options, Futures, and Other Derivatives (11th ed.). Pearson Educational Limited. Copyright.

Glasserman, P. (2013). Monte Carlo Methods in Financial Engineering. Springer Science & Business Media.

Glasserman, P. (2004). Monte Carlo Methods in Financial Engineering, Section 3.2.. Springer Science & Business Media.

9 Appendix

9.1 Derivation of Greeks for Pathwise Estimators

$$Y = e^{-rT}[\bar{S} - K]^+ \bar{S} = \frac{1}{m}\sum_{i=1}^{m} S_{t_i}$$

$$S_t = S_0 e^{(r-\frac{1}{2}\sigma^2)t+\sigma W_t}$$

$$\implies \bar{S} = \frac{1}{m}\sum_{i=1}^{m} S_{t_i} = \frac{1}{m}\sum_{i=1}^{m} S_0 e^{(r-\frac{1}{2}\sigma^2)t_i+\sigma W_{t_i}} = \frac{1}{m} S_0 \sum_{i=1}^{m} e^{(r-\frac{1}{2}\sigma^2)t_i+\sigma W_{t_i}}$$

9.1.1 Delta

$$\frac{\partial Y}{\partial S_0} = \frac{\partial Y}{\partial \bar{S}}\frac{\partial \bar{S}}{\partial S_0}$$

$$\frac{\partial Y}{\partial \bar{S}} = \frac{\partial}{\partial \bar{S}}[e^{-rT}[\bar{S} - K]^+] = e^{-rT}\frac{\partial}{\partial \bar{S}}[[\bar{S} - K]^+] = e^{-rT} 1\{\bar{S} > K\}$$

$$\frac{\partial \bar{S}}{\partial S_0} = \frac{\partial}{\partial S_0}[\frac{1}{m} S_0 \sum_{i=1}^{m} e^{(r-\frac{1}{2}\sigma^2)t_i+\sigma W_{t_i}}] = \frac{1}{m}\sum_{i=1}^{m} e^{(r-\frac{1}{2}\sigma^2)t_i+\sigma W_{t_i}} = \frac{\bar{S}}{S_0}$$

$$\implies \frac{\partial Y}{\partial S_0} = \frac{\partial Y}{\partial \bar{S}}\frac{\partial \bar{S}}{\partial S_0} = e^{-rT} 1\{\bar{S} > K\}\frac{\bar{S}}{S_0}$$

$$\boxed{\frac{\partial Y}{\partial S_0} = e^{-rT} 1\{\bar{S} > K\}\frac{\bar{S}}{S_0}}$$

9.1.2 Vega

$$
\begin{aligned}
\frac{\partial Y}{\partial \sigma} &= \frac{\partial Y}{\partial \bar{S}} \frac{\partial \bar{S}}{\partial \sigma} \\
\frac{\partial Y}{\partial \bar{S}} &= \frac{\partial}{\partial \bar{S}} [e^{-rT} [\bar{S} - K]^+] \\
&= e^{-rT} \frac{\partial}{\partial \bar{S}} [[\bar{S} - K]^+] \\
&= e^{-rT} 1\{\bar{S} > K\} \\
\frac{\partial \bar{S}}{\partial \sigma} &= \frac{\partial}{\partial \sigma} [\frac{1}{m} S_0 \sum_{i=1}^{m} e^{(r - \frac{1}{2}\sigma^2)t_i + \sigma W_{t_i}}] \\
&= \frac{1}{m} S_0 \sum_{i=1}^{m} \frac{\partial}{\partial \sigma} [e^{(r - \frac{1}{2}\sigma^2)t_i + \sigma W_{t_i}}] \\
&= \frac{1}{m} S_0 \sum_{i=1}^{m} e^{(r - \frac{1}{2}\sigma^2)t_i + \sigma W_{t_i}} [-\sigma t_i + W_{t_i}] \\
\implies \frac{\partial Y}{\partial \sigma} &= \frac{\partial Y}{\partial \bar{S}} \frac{\partial \bar{S}}{\partial \sigma} = e^{-rT} 1\{\bar{S} > K\} \frac{1}{m} S_0 \sum_{i=1}^{m} e^{(r - \frac{1}{2}\sigma^2)t_i + \sigma W_{t_i}} [-\sigma t_i + W_{t_i}]
\end{aligned}
$$

$$
\boxed{\frac{\partial Y}{\partial \sigma} = e^{-rT} 1\{\bar{S} > K\} \frac{1}{m} S_0 \sum_{i=1}^{m} e^{(r - \frac{1}{2}\sigma^2)t_i + \sigma W_{t_i}} [-\sigma t_i + W_{t_i}]}
$$

9.1.3 Rho

Since r is in $\bar{S}$, as well as e^{-rT}, product rule is needed.
Let:

$$
\begin{aligned}
f(r) &= e^{-rT} \\
g(r) &= [\bar{S} - K]^+
\end{aligned}
$$

We are calculating

$$
\frac{\partial Y}{\partial r} = \frac{\partial f(r)}{\partial r} g(r) + f(r) \frac{\partial g(r)}{\partial r}
$$

Thus

$$\frac{\partial f(r)}{\partial r} = -Te^{-rT}$$
$$\frac{\partial g(r)}{\partial r} = \frac{\partial g(r)}{\partial \bar{S}}\frac{\partial \bar{S}}{\partial r}$$
$$\frac{\partial g(r)}{\partial \bar{S}} = \frac{\partial}{\partial \bar{S}}[[\bar{S}-K]^+] = 1\{\bar{S}>K\}$$
$$\frac{\partial \bar{S}}{\partial r} = \frac{\partial}{\partial r}[\frac{1}{m}S_0\sum_{i=1}^{m} e^{(r-\frac{1}{2}\sigma^2)t_i+\sigma W_{t_i}}] = \frac{1}{m}S_0\sum_{i=1}^{m}\frac{\partial}{\partial r}[e^{(r-\frac{1}{2}\sigma^2)t_i+\sigma W_{t_i}}] = \frac{1}{m}S_0\sum_{i=1}^{m} t_i e^{(r-\frac{1}{2}\sigma^2)t_i+\sigma W_{t_i}}$$
$$\implies \frac{\partial g(r)}{\partial r} = \frac{\partial g(r)}{\partial \bar{S}}\frac{\partial \bar{S}}{\partial r} = 1\{\bar{S}>K\}\frac{1}{m}S_0\sum_{i=1}^{m} t_i e^{(r-\frac{1}{2}\sigma^2)t_i+\sigma W_{t_i}}$$

Finally

$$\frac{\partial Y}{\partial r} = \frac{\partial f(r)}{\partial r}g(r) + f(r)\frac{\partial g(r)}{\partial r} = -Te^{-rT}[\bar{S}-K]^+ + e^{-rT}1\{\bar{S}>K\}\frac{1}{m}S_0\sum_{i=1}^{m} t_i e^{(r-\frac{1}{2}\sigma^2)t_i+\sigma W_{t_i}}$$

$$\boxed{\frac{\partial Y}{\partial r} = e^{-rT}[-T[\bar{S}-K]^+ + 1\{\bar{S}>K\}\frac{1}{m}S_0\sum_{i=1}^{m} t_i e^{(r-\frac{1}{2}\sigma^2)t_i+\sigma W_{t_i}}]}$$

9.2 Derivation of Closed form formula for the geometric average Asian call option

Want to show:

$$\left(\prod_{i=1}^{m} S(t_i)\right)^{1/m} = S_0 \exp\left[\left(r-\tfrac{1}{2}\sigma^2\right)\frac{1}{m}\sum_{i=1}^{m} t_i + \frac{\sigma}{m}\sum_{i=1}^{m} W(t_i)\right]$$

Since we have:

$$S_{t_i} = S_0 \exp\left((r-\tfrac{1}{2}\sigma^2)t_i + \sigma W(t_i)\right)$$

and

$$\bar{S} = \left(\prod_{i=1}^{m} S_{t_i}\right)^{1/m}$$

Then

$$\begin{aligned}\bar{S} &= \left(\prod_{i=1}^{m} S_{t_i}\right)^{1/m} \\ &= \left(\prod_{i=1}^{m} S_0 \exp\left((r-\tfrac{1}{2}\sigma^2)t_i + \sigma W(t_i)\right)\right)^{1/m}\end{aligned}$$

Thus,

$$\prod_{i=1}^{m} S_0 \exp\left((r-\tfrac{1}{2}\sigma^2)t_i + \sigma W(t_i)\right) = S_0^m \prod_{i=1}^{m} \exp\left((r-\tfrac{1}{2}\sigma^2)t_i + \sigma W(t_i)\right)$$

Use $\prod e^{a_i} = e^{\sum a_i}$, we would have:

$$\prod_{i=1}^{m} \exp\left((r-\tfrac{1}{2}\sigma^2)t_i + \sigma W(t_i)\right) = \exp\left(\sum_{i=1}^{m}\left((r-\tfrac{1}{2}\sigma^2)t_i + \sigma W(t_i)\right)\right)$$

Then,

$$\bar{S} = \left(S_0^m \exp\left(\sum_{i=1}^{m}\left((r-\tfrac{1}{2}\sigma^2)t_i + \sigma W(t_i)\right)\right)\right)^{1/m}$$

After this, we are going to take $1/m$ off the equation:

$$\bar{S} = S_0 \exp\left(\frac{1}{m}\sum_{i=1}^{m}\left((r-\tfrac{1}{2}\sigma^2)t_i + \sigma W(t_i)\right)\right)$$

Finally, we will have:

$$\bar{S} = S_0 \exp\left[\left(r-\tfrac{1}{2}\sigma^2\right)\frac{1}{m}\sum_{i=1}^{m} t_i + \frac{\sigma}{m}\sum_{i=1}^{m} W(t_i)\right]$$

as needed. □

9.3 Derivation of covariance structure for the Brownian motion sum

Want to show:

$$\sum_{i=1}^{m} W(t_i) \sim N\left(0,\ \sum_{i=1}^{m}(2i-1)\, t_{m+1-i}\right)$$

where $0 < t_1 < t_2 < \cdots < t_m$ and $\{W(t)\}_{t\geq 0}$ is a standard Brownian motion. Let

$$S := \sum_{i=1}^{m} W(t_i)$$

Since $(W(t_1), \ldots, W(t_m))$ is jointly normal, any linear combination of these random variables is normal. Therefore S is normally distributed.

Moreover, for each i we have $\mathbb{E}[W(t_i)] = 0$, so

$$\mathbb{E}[S] = \mathbb{E}\left[\sum_{i=1}^{m} W(t_i)\right] = \sum_{i=1}^{m} \mathbb{E}[W(t_i)] = 0$$

Thus S is a mean–zero normal random variable, and it remains to compute its variance.

By definition of variance of a sum,

$$Var(S) = Var\left(\sum_{i=1}^{m} W(t_i)\right) = \sum_{i=1}^{m}\sum_{j=1}^{m} Cov\big(W(t_i), W(t_j)\big)$$

For Brownian motion we know that

$$Cov\big(W(t_i), W(t_j)\big) = \min(t_i, t_j)$$

so

$$Var(S) = \sum_{i=1}^{m}\sum_{j=1}^{m} \min(t_i, t_j)$$

We now simplify this double sum. Split it into diagonal, upper–triangular and lower–triangular parts:

$$\sum_{i=1}^{m}\sum_{j=1}^{m} \min(t_i, t_j) = \sum_{i=1}^{m} \min(t_i, t_i) + \sum_{1\leq i<j\leq m} \min(t_i, t_j) + \sum_{1\leq j<i\leq m} \min(t_i, t_j)$$

Since $t_1 < \cdots < t_m$, we have

$$\min(t_i, t_i) = t_i, \quad \min(t_i, t_j) = t_i \text{ for } i < j, \quad \min(t_i, t_j) = t_j \text{ for } j < i.$$

Hence

$$Var(S) = \sum_{i=1}^{m} t_i + \sum_{1 \le i < j \le m} t_i + \sum_{1 \le j < i \le m} t_j$$

The last two sums are equal by symmetry (rename indices), so

$$Var(S) = \sum_{i=1}^{m} t_i + 2 \sum_{1 \le i < j \le m} t_i$$

Write the second term more explicitly:

$$\sum_{1 \le i < j \le m} t_i = \sum_{i=1}^{m-1} \sum_{j=i+1}^{m} t_i = \sum_{i=1}^{m-1} (m-i)\, t_i$$

Therefore

$$\begin{aligned} Var(S) &= \sum_{i=1}^{m} t_i + 2 \sum_{i=1}^{m-1} (m-i)\, t_i \\ &= \sum_{i=1}^{m-1} \big[1 + 2(m-i)\big]\, t_i + t_m \end{aligned}$$

Notice that for $i = m$ we also have $1 + 2(m-i) = 1$, so

$$Var(S) = \sum_{i=1}^{m} \big[1 + 2(m-i)\big]\, t_i$$

Now simplify it:

$$1 + 2(m-i) = 2m - 2i + 1$$

Thus,

$$Var(S) = \sum_{i=1}^{m} (2m - 2i + 1)\, t_i$$

Finally, let $k = m + 1 - i$, so $i = m + 1 - k$. Then

$$Var(S) = \sum_{k=1}^{m} \big[2k - 1\big]\, t_{m+1-k} = \sum_{i=1}^{m} (2i - 1)\, t_{m+1-i}$$

Hence

$$S = \sum_{i=1}^{m} W(t_i) \sim N\left(0,\ \sum_{i=1}^{m}(2i-1)\, t_{m+1-i}\right)$$

as needed. □

9.4 Derivation of the adjusted volatility $\bar{\sigma}^2$

Want to show:

$$\bar{\sigma}^2 = \frac{\sigma^2}{m^2 \bar{T}} \sum_{i=1}^{m}(2i-1)\, t_{m+1-i},$$

where

$$\bar{T} = \frac{1}{m}\sum_{i=1}^{m} t_i, \qquad \sum_{i=1}^{m} W(t_i) \sim N\left(0,\ \sum_{i=1}^{m}(2i-1) t_{m+1-i}\right).$$

From the geometric average derivation, we have

$$\bar{S} = S_0 \exp\left[\left(r - \tfrac{1}{2}\sigma^2\right)\frac{1}{m}\sum_{i=1}^{m} t_i + \frac{\sigma}{m}\sum_{i=1}^{m} W(t_i)\right].$$

Using the definition of $\bar{T}$, this becomes

$$\bar{S} = S_0 \exp\left[\left(r - \tfrac{1}{2}\sigma^2\right)\bar{T} + \frac{\sigma}{m}\sum_{i=1}^{m} W(t_i)\right],$$

so that

$$\log \bar{S} = \log S_0 + \left(r - \tfrac{1}{2}\sigma^2\right)\bar{T} + \frac{\sigma}{m}\sum_{i=1}^{m} W(t_i).$$

The random part is

$$\frac{\sigma}{m}\sum_{i=1}^{m} W(t_i),$$

and since

$$Var\left(\sum_{i=1}^{m} W(t_i)\right) = \sum_{i=1}^{m}(2i-1) t_{m+1-i},$$

we get

$$Var\left(\frac{\sigma}{m}\sum_{i=1}^{m}W(t_i)\right) = \frac{\sigma^2}{m^2}Var\left(\sum_{i=1}^{m}W(t_i)\right)$$
$$= \frac{\sigma^2}{m^2}\sum_{i=1}^{m}(2i-1)t_{m+1-i}.$$

To apply Black-Scholes,We denote this equivalent GBM value by D_T:

$$D_T = S_0 \exp\big((r-\delta-\tfrac{1}{2}\bar{\sigma}^2)\,\bar{T}\ +\ \bar{\sigma}W_{\bar{T}}\big)\,.$$

Since the exponent is affine in brownian motion, log is normally distributed:

$$\log D_T \sim N\big(\log S_0 + (r-\delta-\tfrac{1}{2}\bar{\sigma}^2)\bar{T},\ \bar{\sigma}^2\,\bar{T}\big)\,.$$

Therefore,

$$\bar{\sigma}^2\bar{T} = \frac{\sigma^2}{m^2}\sum_{i=1}^{m}(2i-1)t_{m+1-i}.$$

Solving for $\bar{\sigma}^2$

$$\boxed{\bar{\sigma}^2 = \frac{\sigma^2}{m^2\bar{T}}\sum_{i=1}^{m}(2i-1)t_{m+1-i},}$$

as needed. □

9.5 Derivation of the adjusted dividend yield δ

Want to show:

$$\delta = \frac{1}{2}\sigma^2 - \frac{1}{2}\bar{\sigma}^2$$

where $\bar{\sigma}^2$ is the adjusted volatility obtained above and $\bar{T} = \frac{1}{m}\sum_{i=1}^{m} t_i$.

From the geometric average, we have

$$\log \bar{S} = \log S_0 + \big(r - \tfrac{1}{2}\sigma^2\big)\,\bar{T} + \frac{\sigma}{m}\sum_{i=1}^{m}W(t_i)$$

Hence the mean of $\log \bar{S}$ is

$$\mathbb{E}[\log \bar{S}] = \log S_0 + \big(r - \tfrac{1}{2}\sigma^2\big)\,\bar{T}$$

We now model $\bar{S}$ as the value at time $\bar{T}$ of a GBM with drift $r-\delta$ and volatility $\bar{\sigma}$:

$$D_T = S_0 \exp\left((r-\delta-\tfrac{1}{2}\bar{\sigma}^2)\bar{T} + \bar{\sigma}W(\bar{T})\right)$$

Taking expectations:

$$\mathbb{E}[\log D_T] = \log S_0 + (r-\delta-\tfrac{1}{2}\bar{\sigma}^2)\bar{T}$$

then,

$$\log S_0 + \left(r-\tfrac{1}{2}\sigma^2\right)\bar{T} = \log S_0 + (r-\delta-\tfrac{1}{2}\bar{\sigma}^2)\bar{T}$$

Cancel $\log S_0$ and divide both sides by $\bar{T} > 0$,

$$r-\tfrac{1}{2}\sigma^2 = r-\delta-\tfrac{1}{2}\bar{\sigma}^2$$

Therefore we have,

$$\begin{aligned} -\tfrac{1}{2}\sigma^2 &= -\delta-\tfrac{1}{2}\bar{\sigma}^2 \\ \delta &= \tfrac{1}{2}\sigma^2-\tfrac{1}{2}\bar{\sigma}^2 \end{aligned}$$

as required.□

9.6 Derivation of d_+ and d_- for the geometric average Asian call

Want to show:

$$d_+ = \frac{\ln(S_0/K) + (r-\delta+\tfrac{1}{2}\bar{\sigma}^2)\,\bar{T}}{\bar{\sigma}\sqrt{\bar{T}}}, \qquad d_- = d_+ - \bar{\sigma}\sqrt{\bar{T}}.$$

From the previous derivation, the geometric average can be represented as the value at time $\bar{T}$ of a GBM with drift $r-\delta$ and volatility $\bar{\sigma}$. We denote this equivalent GBM value by D_T:

$$D_T = S_0 \exp\Big((r-\delta-\tfrac{1}{2}\bar{\sigma}^2)\bar{T} + \bar{\sigma}W_{\bar{T}}\Big).$$

Taking logarithms, we obtain

$$\log D_T = \log S_0 + (r-\delta-\tfrac{1}{2}\bar{\sigma}^2)\bar{T} + \bar{\sigma}W_{\bar{T}}.$$

Since $W_{\bar{T}} \sim N(0,\bar{T})$, it follows that

$$\log D_T \sim N(\mu_L, \sigma_L^2),$$

where

$$\mu_L = \log S_0 + (r - \delta - \tfrac{1}{2}\bar{\sigma}^2)\bar{T}, \qquad \sigma_L^2 = \bar{\sigma}^2 \bar{T}.$$

The price of the call option on the geometric average is

$$C_0 = e^{-r\bar{T}}\,\mathbb{E}\big[(D_T - K)^+\big].$$

Let $X = \log D_T$, so that $D_T = e^X$ and $X \sim N(\mu_L, \sigma_L^2)$. Then

$$\begin{aligned} C_0 &= e^{-r\bar{T}}\,\mathbb{E}\big[(e^X - K)^+\big] \\ &= e^{-r\bar{T}} \int_{\ln K}^{\infty} (e^x - K)\, f_X(x)\,\mathrm{d}x, \end{aligned}$$

where f_X is the density of $N(\mu_L, \sigma_L^2)$:

$$f_X(x) = \frac{1}{\sqrt{2\pi}\sigma_L} \exp\left(-\frac{(x-\mu_L)^2}{2\sigma_L^2}\right).$$

Standardize X by defining

$$Z = \frac{X - \mu_L}{\sigma_L} = \frac{X - \mu_L}{\bar{\sigma}\sqrt{\bar{T}}}, \qquad Z \sim N(0,1).$$

The lower bound $x = \ln K$ corresponds to

$$z_K = \frac{\ln K - \mu_L}{\bar{\sigma}\sqrt{\bar{T}}}.$$

We first compute the term involving e^x:

$$\begin{aligned} e^{-r\bar{T}} \int_{\ln K}^{\infty} e^x f_X(x)\,\mathrm{d}x &= e^{-r\bar{T}} \int_{z_K}^{\infty} \exp\big(\mu_L + \sigma_L z\big) \frac{1}{\sqrt{2\pi}} e^{-z^2/2}\,\mathrm{d}z \\ &= e^{-r\bar{T}} e^{\mu_L} \int_{z_K}^{\infty} \exp\left(\sigma_L z - \frac{z^2}{2}\right) \frac{\mathrm{d}z}{\sqrt{2\pi}}. \end{aligned}$$

Completing the square:

$$\sigma_L z - \frac{z^2}{2} = \frac{\sigma_L^2}{2} - \frac{1}{2}(z - \sigma_L)^2.$$

Thus

$$e^{-r\bar{T}}e^{\mu_L+\sigma_L^2/2} = S_0 e^{-\delta\bar{T}}.$$

Define

$$d_+ := \frac{\ln(S_0/K) + (r - \delta + \frac{1}{2}\bar{\sigma}^2)\bar{T}}{\bar{\sigma}\sqrt{\bar{T}}},$$

so that

$$1 - \Phi(z_K - \sigma_L) = \Phi(d_+).$$

The second term becomes

$$e^{-r\bar{T}}K[1 - \Phi(z_K)] = Ke^{-r\bar{T}}\Phi(d_-),$$

with

$$d_- := d_+ - \bar{\sigma}\sqrt{\bar{T}}.$$

Putting the pieces together:

$$\boxed{C_0 = S_0 e^{-\delta\bar{T}}\Phi(d_+) - Ke^{-r\bar{T}}\Phi(d_-)},$$

with

$$\boxed{d_+ = \frac{\ln(S_0/K) + (r - \delta + \frac{1}{2}\bar{\sigma}^2)\bar{T}}{\bar{\sigma}\sqrt{\bar{T}}}, \qquad d_- = d_+ - \bar{\sigma}\sqrt{\bar{T}}},$$

as needed. □

9.7 Derivation of the pricing formula for barrier up-and-in put option

We derive the price of an up-and-in European put with strike K and up-barrier H under the Black-Scholes model with continuous dividend yield q. For convenience, we will use the following payoff function instead, which is equivalent to the one in section 7:

$$(K - S_T)_+ \, \mathbb{I}_{\{M_T \geq H\}}.$$

We assume $S_0 < H$ and $H \geq K$.

1. Risk-neutral dynamics and the option payoff

Under the risk-neutral measure $\mathbb{Q}$, the asset follows

$$dS_t = (r - q)S_t \, dt + \sigma S_t \, dW_t^{\mathbb{Q}}.$$

Let $M_T = \max_{0 \leq u \leq T} S_u$. An up-and-in put has payoff

$$(K - S_T)_+ \, \mathbf{1}_{\{M_T \geq H\}}.$$

Hence its price at $t = 0$ is:

$$p_{\text{ui}} = e^{-rT} \, \mathbb{E}^{\mathbb{Q}}\left[(K - S_T)_+ \, \mathbb{I}_{\{M_T \geq H\}}\right]. \tag{4}$$

2. In-out parity

For fixed (K, H, T),

$$p_{\text{vanilla}} = p_{\text{ui}} + p_{\text{uo}},$$

where p_{uo} is the price of the corresponding up-and-out put. Thus

$$p_{\text{ui}} = p_{\text{vanilla}} - p_{\text{uo}}. \tag{5}$$

The Black–Scholes vanilla European put price p_{vanilla} is known, so it remains to compute p_{uo}.

3. Log-price transformation and the reflection principle

Set

$$X_t = \ln S_t, \qquad x_0 = \ln S_0, \qquad h = \ln H.$$

By Ito's formula,

$$X_t = x_0 + \left(r - q - \tfrac{1}{2}\sigma^2\right) t + \sigma W_t^{\mathbb{Q}},$$

so

$$X_T \sim N(m, s^2), \qquad m = x_0 + (r - q - \tfrac{1}{2}\sigma^2)T, \quad s^2 = \sigma^2 T.$$

Let $f_{\text{plain}}(x)$ denote this Gaussian density.

A standard result from the reflection principle for Brownian motion with drift states that for $x < h$,

$$f_{\text{no-hit}}(x) = f_{\text{plain}}(x) - \left(\frac{H}{S_0}\right)^{2\lambda-2} f_{\text{plain}}(2h - x), \tag{6}$$

where

$$\lambda = \frac{r - q + \frac{1}{2}\sigma^2}{\sigma^2}.$$

Since the put pays only when $S_T < K \leq H$, we only require the density on $(-\infty, \ln K)$.

4. Integral formula for the up-and-out put

An up-and-out put pays only if $M_T < H$ and $S_T < K$:

$$p_{\text{uo}} = e^{-rT} \int_{-\infty}^{\ln K} (K - e^x)\, f_{\text{no-hit}}(x)\, dx.$$

Using (6),

$$\begin{aligned} p_{\text{uo}} = e^{-rT} &\int_{-\infty}^{\ln K} (K - e^x) f_{\text{plain}}(x)\, dx \\ &- e^{-rT} \left(\frac{H}{S_0}\right)^{2\lambda-2} \int_{-\infty}^{\ln K} (K - e^x) f_{\text{plain}}(2h - x)\, dx. \end{aligned} \tag{7}$$

The first integral is exactly the Black-Scholes vanilla put integral:

$$e^{-rT} \int_{-\infty}^{\ln K} (K - e^x) f_{\text{plain}}(x)\, dx = p_{\text{vanilla}}.$$

Define the second integral as

$$I := \int_{-\infty}^{\ln K} (K - e^x) f_{\text{plain}}(2h - x)\, dx.$$

5. Computing the "mirror" integral

Apply the change of variable $z = 2h - x$, so $dx = -dz$ and

$$I = \int_{\ln(H^2/K)}^{\infty} \left(K - e^{2h-z}\right) f_{\text{plain}}(z)\, dz = KA - H^2 B,$$

where

$$A = \int_{\ln(H^2/K)}^{\infty} f_{\text{plain}}(z)\, dz, \qquad B = \int_{\ln(H^2/K)}^{\infty} e^{-z} f_{\text{plain}}(z)\, dz.$$

Since $X_T \sim N(m, s^2)$,

$$A = \Phi\left(-\frac{\ln(H^2/K) - m}{s}\right).$$

Define

$$y := \frac{\ln\left(\frac{H^2}{S_0 K}\right) + (r - q + \frac{1}{2}\sigma^2)T}{\sigma\sqrt{T}} = \frac{\ln(H^2/K) - m}{s},$$

so that $A = \Phi(-y)$.

A standard Gaussian completion-of-squares calculation yields

$$B = \frac{1}{H^2}\left(\frac{H}{S_0}\right)^{2\lambda} e^{(r-q)T}\, \Phi(-y + \sigma\sqrt{T}).$$

Hence

$$I = K\Phi(-y) - \left(\frac{H}{S_0}\right)^{2\lambda} e^{(r-q)T}\Phi(-y + \sigma\sqrt{T}). \tag{8}$$

Substituting (8) into (7), we obtain

$$p_{\text{uo}} = p_{\text{vanilla}} - Ke^{-rT}\left(\frac{H}{S_0}\right)^{2\lambda-2}\Phi(-y) + S_0 e^{-qT}\left(\frac{H}{S_0}\right)^{2\lambda}\Phi(-y + \sigma\sqrt{T}). \tag{9}$$

6. Up-and-in put price

Using in–out parity (5),

$$p_{\text{ui}} = p_{\text{vanilla}} - p_{\text{uo}}.$$

Substituting (9),

$$p_{\text{ui}} = -S_0 e^{-qT}\left(\frac{H}{S_0}\right)^{2\lambda}\Phi(-y) + Ke^{-rT}\left(\frac{H}{S_0}\right)^{2\lambda-2}\Phi(-y + \sigma\sqrt{T}).$$

7. Final closed-form expression

Thus the price of an up-and-in put with $H \geq K$ is

$$\boxed{p_{\text{ui}} = -S_0 e^{-qT} \left(\frac{H}{S_0}\right)^{2\lambda} \Phi(-y) + K e^{-rT} \left(\frac{H}{S_0}\right)^{2\lambda-2} \Phi(-y + \sigma\sqrt{T}),}$$

where

$$\boxed{\lambda = \frac{r - q + \frac{1}{2}\sigma^2}{\sigma^2}, \qquad y = \frac{\ln\left(\frac{H^2}{S_0 K}\right) + (r - q + \frac{1}{2}\sigma^2)T}{\sigma\sqrt{T}}.}$$

which is in alignment with the result in Hull.□